J Comput Neurosci
DOI 10.1007/s10827-015-0588-y

Sensory feedback in a bump attractor model of path integration

Daniel B. Poll[1] · Khanh Nguyen[1] · Zachary P. Kilpatrick[1]

Received: 15 July 2015 / Revised: 14 December 2015 / Accepted: 22 December 2015

Abstract Mammalian spatial navigation systems utilize several different sensory information channels. This information is converted into a neural code that represents the animal's current position in space by engaging place cell, grid cell, and head direction cell networks. In particular, sensory landmark (allothetic) cues can be utilized in concert with an animal's knowledge of its own velocity (idiothetic) cues to generate a more accurate representation of position than path integration provides on its own (Battaglia et al. The Journal of Neuroscience 24(19):4541–4550 (2004)). We develop a computational model that merges path integration with feedback from external sensory cues that provide a reliable representation of spatial position along an annular track. Starting with a continuous bump attractor model, we explore the impact of synaptic spatial asymmetry and heterogeneity, which disrupt the position code of the path integration process. We use asymptotic analysis to reduce the bump attractor model to a single scalar equation whose potential represents the impact of asymmetry and heterogeneity. Such imperfections cause errors to build up when the network performs path integration, but these errors can be corrected by an external control signal representing the

Action Editor: Simon R. Schultz

✉ Zachary P. Kilpatrick
zpkilpat@math.uh.edu

Khanh Nguyen
kpnguyen@math.uh.edu

Daniel B. Poll
dbpoll@math.uh.edu

1

imperfect summation of velocity inputs (Brody et al. 2003). Any inaccuracy in the represented position or velocity will be compounded over time, as the neural code continues to trace the animal's true path (Knierim et al. 1995; Valerio and Taube 2012). Fortunately, path integration is not the sole navigational technique of the mammalian brain; landmarks detected by the sensory system help anchor and correct the integrated velocity signal (Fig. 1a) (Etienne et al. 1996; Collett and Graham 2004; Solstad et al. 2008).

Several experiments have demonstrated that mammals' representation of space is sharpened in the presence of sensory cues (Battaglia et al. 2004; Ulanovsky and Moss 2011; Aikath et al. 2014; Zhang et al. 2014). Experiments typically compare place fields of individuals cells - spatial locations where the cell becomes active - in the presence and absence of sensory landmarks (e.g., steel brush or ticking clock; Fig. 1b). For instance, Battaglia et al. (2004) recorded from hippocampal place cells in rats moving on an annular track. When there were no sensory cues along the track, the measured place field of an individual cell could differ substantially, depending on whether the rat was moving clockwise or counterclockwise around the annulus. This suggests there was some drift in animals' neural representation of their position. However, when several position cues were placed along the track, the clockwise and counterclockwise place fields of individual cells were strongly correlated. This suggests the sensory cues tightened the navigation system's fine representation of the animal's spatial position (Save et al. 2000). Similar effects have been observed in brown bats, whose echolocation signals provide a brief burst of rich sensory information, sharpening the animal's place fields (Ulanovsky and Moss 2011 balance of excitation and inhibition. A similar mechanism was utilized by Burak and Fiete (2009) in a two-dimensional model of grid cell activity. Thus, this framework is a well accepted model of position encoding cells in hippocampus, entorhinal cortex, and the vestibular system (Zhang 1996). Since we are modeling motion along an annulus (Fig. 1b), we have restricted the network to a one-dimensional periodic domain. Sensory cues are assumed to provide a reliable estimate of the animal's true position. This position is then compared with the place cell network's estimate of position. Any discrepancy in the position estimate is then translated into a corrective velocity input, which is added to the baseline velocity input (Fig. 1a). Even when the cues occur discretely in space, this mechanism works well for reducing the long term error in the position estimate.

In Section 2, we introduce the neural field model of spatial navigation, which combines path integration and sensory cue feedback. Next, we derive a low-dimensional approximation for the dynamics of bump position in the neural field model (Section 3). This reduction reveals the relative influence of velocity inputs, sensory feedback, and heterogeneity on the animal's perceived position of its current location. Ultimately, this allows us to calculate the impact of various control strategies on the error between the animal's perceived position and true position (Section 4). Our main finding is that there is an optimal control strength at which the long term error of the network is minimized. Our findings were similar in the case that errors arose due to dynamic noise fluctuations (Section 4.2), rather than synaptic heterogeneities (Section 4.1). In this case, the low-dimensional approximation of the neural field is a stochastic differential equation whose variance we can evaluate explicitly.

2 Sensory control in velocity-integrating place cell networks

We employ a neural field model of velocity integration that sustains a bump attractor of neural activity in the absence of any inputs. Amari (1977) pioneered the scalar neural field model as a reduction of the excitatory-inhibitory model of Wilson and Cowan (1973), but the incorporation of velocity inputs that shift the bump around the spatial domain is more recent. Originally developed as a model of the head direction system (Zhang 1996), velocity-integrating networks introduce an external input that alters the shape of the recurrent architecture (McNaughton et al. 1991). As a result, a moving bump, rather than a stationary bump, becomes the stable solution to the model

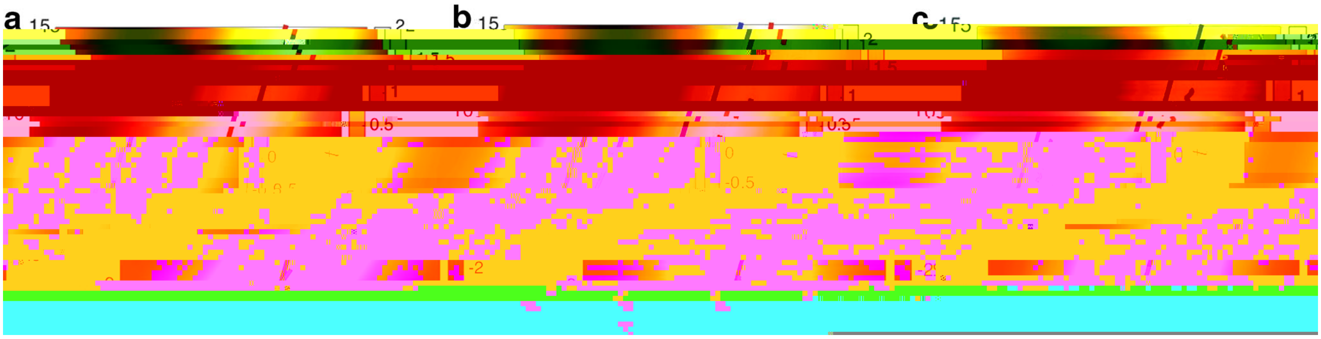

Fig. 2 Velocity-integration with moving bump attractors in the neural field model Eq. (2.1) with a Heaviside firing rate function Eq. (2.8) with threshold $\theta = 0$ and a cosine base weight function $w_0(x) = \cos(x)$. **a** Bump of neural activity $u(x,t)$ perfectly integrates velocity inputs in the case of no heterogeneity ($\sigma = 0$) and no noise ($\epsilon = 0$), showing the animal's true position (solid line) is perfectly tracked by the center of mass of the bump (dashed). **b** In a heterogeneous network ($\sigma = 0.1$ with $w_u = \sin(x)$), the bump initially moves too fast due to a discrete attractor of the input-free system at $x = \pi/2$, so the bump's center of mass is mismatched with the true position of the animal. **c** In the presence of spatiotemporal noise ($\epsilon = 0.2$ with cosine correlations $C(x) = \cos(x)$), the bump wanders diffusively so the encoded position tends to slowly distance itself from the true position. Here the external velocity input is constant $v(t) = 0.1$. Numerical simulations are performed using an Euler timestep with $dt = 0.1$ and a trapezoidal rule on the integral with $dx \approx 0.003$

Thus, assuming a sensory mechanism for correcting the place cell's encoded position when a cue is encountered, take the velocity input to be

$$\bar{v}(t) := v(t) + v_c(t),$$

the sum of the animal's true velocity $v(t)$ and an external control signal $v_c(t)$. This is meant to account for the improved place representation observed when animals can employ information about sensory landmarks (Battaglia et al. 2004; Ulanovsky and Moss 2011; Aikath et al. 2014). As shown in the schematic in Fig. 1a, we assume there is a network that can access the place cell network's perceived position $\Delta(t)$ via a readout of the center of mass of neural activity (Deneve et al. 1999)

$$\Delta(t) = \int_{-\pi}^{\pi} x f(u(x,t))\, dx \tag{2.4}$$

The present positional error is then computed by comparing the perceived position $\Delta(t)$ to the animal's actual position given by a time integral of the velocity input

$$\Delta_T(t) = \int_0^t v(s)\, ds$$

so the error

$$\epsilon(t) = \Delta_T(t) - \Delta(t), \tag{2.5}$$

which will be positive (negative) if the estimated position is to the left (right) of the true position. Note, we extend the domain $x \in [-\pi, \pi]$ to compute Eq. (2.5) in cases where the closest distance between Δ_T and Δ is across the boundary cuts at $x = \pm\pi$. The error $\epsilon(t)$ is then translated either into a continuous velocity control signal

$$v_c(t) = \kappa\epsilon(t) = \kappa \cdot (\Delta_T(t) - \Delta(t)), \tag{2.6}$$

or a discrete control signal given by

$$\frac{dv_c}{dt} = -\frac{v_c(t)}{\tau} + \kappa \sum_{k=1}^{N_c} \epsilon(t_k)\,\delta(t - t_k), \tag{2.7}$$

where sensory cues occur at times t_k and κ and τ determine the strength and time decay of control. As we will show, in the case of continuous control Eq. (2.6), strengthening the sensory feedback κ always leads to a reduction of the error. This is not the case for discrete control Eq. (2.7), since the previous sensory cue at $t_k < t$ becomes less relevant as t increases toward t_{k+1}. One of the main goals of this study is to explore how the spacing between subsequent cues $t_{k+1} - t_k$ determines how strong κ the control signal should be.

The nonlinearity f is a firing rate function taken to be sigmoidal (Wilson and Cowan 1973)

$$f(u) := \frac{1}{1 + e^{-\gamma(u-\theta)}},$$

where γ is the gain and θ is the firing threshold. For ease in analysis, we will often consider the high gain limit $\gamma \to \infty$ so that f becomes a Heaviside step function of the form

$$f(u) := H(u - \theta) = \begin{cases} 1 : u \geq \theta, \\ 0 : u < \theta. \end{cases} \tag{2.8}$$

Lastly, we also will consider the impact of the additive noise increment $dW(x,t)$. Spatially extended Langevin equations of the form Eq. (2.1) have become a common model of the effects of fluctuations in large-scale neuronal networks (Bressloff 2012). The noise term is a spatially filtered spatiotemporal white noise process

$$dW(x,t) := \int_{-\pi}^{\pi} F(x - y)\, dY(y,t)\, dy$$

where F is the spatial filter and $dY(x,t)$ is a spatially and temporally white noise increment. With these definitions, the mean and variance can be calculated as $\langle dW(x,t) \rangle = 0$ and $\langle dW(x,t)\, dW(y,s) \rangle = C(x - y)(t - s)\, dt\, d$

3.1 Stationary bump solutions to the translation symmetric network

We begin by assuming the homogeneous connectivity function $w_0(x)$ in Eq. (2.2) satisfies evenness (w

Now plugging in our requirement that the velocity portion of the weight function $w_v(x) = -w_0'(x)$, we have

$$-cU'(\;) + U(\;) = -v_0 \,{}_{-}\, w_0'(\; - y) f(U(y))\, dy$$

$$+ \,{}_{-}\, w_0(\; - y) f(U(y))\, dy \qquad (3.6)$$

Under the assumption that the function $U(\;)$ satisfies the equality Eq. (3.23.2

where we have applied the Eq. (3.7). We can simplify the Eq. (3.12) further by isolating $d(t)$ to yield the stochastic differential equation

$$d(t) = [F((t)) + v(t) + v_c(t) +]dt + dW(t), \quad (3.13)$$

where the impact of synaptic spatial heterogeneities is described by the nonlinear function

$$F() = -\frac{\int f'(U(x))U'(x)\int w_u(y+)w_0(x-y)f(U(y))dydx}{\int f'(U(x))U'(x)^2dx}, \quad (3.14)$$

and the noise term has been projected to a temporal white noise process $W(t)$ with mean zero ($\langle W(t)\rangle = 0$) and variance $\langle W(t)^2\rangle = Dt$ with associated diffusion coefficient

$$D = {}^2\frac{\int\int f'(U(x))U'(x)f'(U(y))U'(y)C(x-y)dydx}{\left[\int f'(U(x))U'(x)^2dx\right]^2}. \quad (3.15)$$

Setting $v_c(t) \equiv 0$ and $v(t) \equiv v_0$ (constant), the dynamics of

Fig. 4 The low-dimensional Eq. (3.13) for the bump position (t) provides an accurate approximation of the bump's movement in the full neural field model Eq. (2.1). **a** Perfect integration of the constant velocity input $v(t) = 0.05$ leads to a constantly drifting bump (solid line) whose position is well approximated by the projected variable (t) (dashed line). Inset shows the tilted potential $V( )$ resulting from the constant velocity input. Circles provide corresponding locations between the two plots at $t = 10, 20, 30$. **b** Spatial heterogeneity $w_u(x) = \sin(x)$ with $= 0.1$ causes bumps to drift toward local attractors of the network. Inset shows potential with a local minimum to which the trajectory is attracted. **c** Spatial heterogeneity $w_u(x) = \sin(6x)$ with $= 0.2$ leads to a more rapid oscillation in the trajectory (t). **d** Spatial heterogeneity $w_u(x) = \sin(4x) + \cos(8x)$ with $= 0.1$ leads to a less regular deviation in the trajectory (t). Heaviside firing rate function Eq. (2.8) has threshold $= 0$. Numerical simulations are run using the same parameters as in Fig. 2

general formulas for all equilibria of Eq. (3.22) are given by

$$\bar{\ }_{k+} = \frac{2k}{m} + \frac{1}{m}\sin^{-1}\frac{v_0}{\ }, \quad k = 0,\dots,m-1, \tag{3.24}$$

$$\bar{\ }_{k-} = \frac{(2k+1)}{m} - \frac{1}{m}\sin^{-1}\frac{v_0}{\ }, \quad k = 0,\dots,m-1. \tag{3.25}$$

On the other hand, when $|\ | < |v_0|$, the heterogeneity $F( )$ will not lead to pinning of bumps, so bumps will propagate

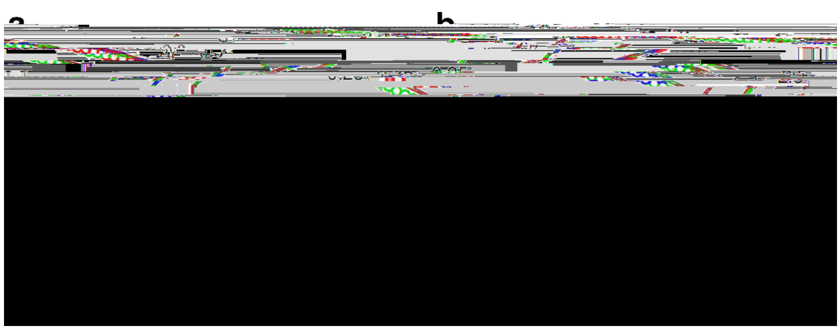

Fig. 5 Spatial heterogeneity slows and even stops the propagation of velocity-driven bumps. **a** Bump position (t) demonstrates the vari-

indefinitely in response to velocity inputs. However, the heterogeneity will ultimately reduce the speed of propagation

Fig. 8 Average error $\langle |r(t)| \rangle$ as a function of time in a heterogeneous network ($w_u(x) = {}_1 \cos(x)$) with control. Velocity-input is constant $v(t) = v_0 = 0.05$. **a** Numerical simulations (dashed lines) of the neural field Eq. (2.1) are well matched by the low-dimensional approximation (solid lines) given by Eq. (4.9). As demonstrated, continuous

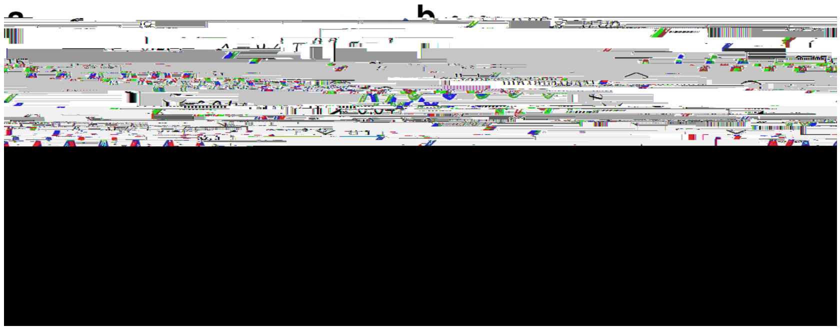

Fig. 9 Variance $\langle \Delta(t)^2 \rangle - \langle \Delta(t) \rangle^2$ computed for the noise-driven network with control. Velocity-input is constant $v(t) = v_0 = 0$. **a** Numerical simulations (dashed lines) of the neural field model Eq. (2.1) are well matched to low-dimensional approximation (solid lines) given by Eq. (4.11). Continuous control substantially reduces the variance, but discrete control with $t = 4$ also provide a variance reduction. Notably, the variance saturates in the case of discrete control as well. **b** Similar to the case of quenched variability through heterogeneity in Fig. 8, varying the strength and timescale of control alters the long term variance. Other parameters are $= 0.2$ and $= 0.1$. Numerical simulations are run with the same parameters as in Fig. 2 with 1000 realizations each curve

model's position estimate. This pattern holds when errors originate from spatial heterogeneities as well as dynamic fluctuations.

Our analysis has focused on one-dimensional periodic systems, wherein it is assumed the animal is navigating along a narrow annular track (Fig. 1b). This was based on the protocol used in the experiments of Battaglia et al. (2004), which were used to study the effect of local cues on the sharpness of neuronal place fields. However, there are several studies of navigation in two-dimensional and even three-dimensional space that demonstrate mammals' ability to use sensory cues to perform error correction (Geva-Sagiv et al. 2015; Solstad et al. 2008). For instance, a recent study has demonstrated that encounters with the boundaries of rectangular environments correct for the systematic drift in position representation (Hardcastle et al. 2015). In particular, border cells in medial entorhinal cortex (MEC) are thought to provide inputs to position-encoding grid cells when an animal senses an environmental boundary. Such recent studies are consistent with the predictions of planar models of spatial navigation based on the dynamics of velocity-driven bump attractors (Burak and Fiete 2009; Samsonovich and McNaughton 1997). The model we have presented here could be extended to incorporate the effects of position-dependent cues, like boundaries, in two-dimensional domains. We expect the extension to two-dimensional neural field models should be possible through a similar negative feedback control mechanism to those presented in Section 2. Our derivation of the reduced equation would then simply yield a position variable that is two-dimensional, with a correction term along each coordinate.

In this work, we have modeled the effects of sensory feedback assuming the distance between an animal's perceived and actual position is relatively small. However, there is also evidence that place cell networks can respond to abrupt and large changes in an animal's spatial context (Wills et al. 2005). In a study by Jezek et al. l.015329-351549e.y the two possible environment representations before settling on the new contextual representation. We could extend our model to account for these observations by exploring the effects of large and strong sensory feedback cues, which could lead to such winner-take-all dynamics (Shpiro et al. 2007; Kilpatrick 2013). There is also recent experimental evidence for discrete, rather than continuous, representations of spatial position by navigational networks. Studying the dynamics of sharp-wave ripple events in hippocampus, Pfeiffer and Foster (2015) showed that reactivation sequences had activity reflecting discrete attractors of the underlying network. Rather than evolving smoothly, neural activity would temporarily sharpen in the vicinity of each position-representing attractor before transitioning to a spatially discontiguous location. In this paradigm, theta or gamma frequency oscillations of inhibitory input could temporarily destabilize attractors, allowing neural activity to traverse the network to subsequent attractors (Welday et al. 2011; Hasselmo and Brandon 2012). It would be interesting to consider such modifications to our model and explore how they impact the robustness of the spatial position code.

We also note that there is recent evidence that the position of discrete objects in the environment may be encoded by cells in the lateral entorhinal cortex (LEC) (Tsao et al. 2013). In particular, these cells tend to be inactive in open environments with no spatial landmarks, but they become active in the presence of objects that can help animals to orient themselves (Deshmukh and Knierim 2011). Some cells in LEC, object-trace cells, have been shown to fire when an animal encounters a location where an object was previously located, demonstrating a persistent memory of location (Tsao et al. 2013). If in fact such cells provide inputs to the position-encoding networks in MEC or hippocampus, LEC object cells could provide a candidate mechanism for the sensory feedback control we have modeled here.

Acknowledgments A

Hasselmo, M.E., & Brandon, M.P. (2012). A model combining oscillations and attractor dynamics for generation of grid cell firing. Front Neural Circuits